Preprints (www.preprints.org) | NOT PEER-REVIEWED | Posted: 1 April 2020 doi:10.20944/preprints202004.0003.v1

Computational screening for potential drug candidates against SARS-CoV-2 main protease

Bruno Silva Andrade[1], Preetam Ghosh[2], Debmalya Barth[3], Sandeep Tiwari[4], Raner José Santana Silva[5], Wagner Rodrigues de Assis Soares[6], Tarcisio Silva Melo[1], Andria dos Santos Freitas[5], Patrícia González-Grande[5], Lucas Sousa Palmeira[1], Luiz Carlos Junior Alcantara[8], Marta Giovanetti[4, 8], Aristóteles Góes-Neto[7], Vasco Ariston de Carvalho Azevedo[4]

[1] Laboratório de Bioinformática e Química Computacional, Departamento de Ciências Biológicas, Universidade Estadual do Sudoeste da Bahia (UESB), Jequié, Bahia, Brazil.
[2]Department of Computer Science, Virginia Commonwealth University, Richmond, VA-23284, USA
[3]Centre for Genomics and Applied Gene Technology, Institute of Integrative Omics and Applied Biotechnology (IIOAB), Purba Medinipur, India
[4]Laboratório de Genética Celular e Molecular, Departamento de Biologia Geral, Instituto de Ciências Biológicas, Universidade Federal de Minas Gerais, Belo Horizonte, Minas Gerais, Brazil.
[5]Programa de Pós-graduação em Genética e Biologia Molecular, Universidade Estadual de Santa Cruz, Ilhéus, Bahia, Brazil.
[6]Universidade Estadual do Sudoeste da Bahia. Departamento de Saúde II. Jequié, Bahia, Brasil.
[7]Laboratório de Biologia Molecular e Computacional de Fungos, Departamento de Microbiologia, Instituto de Ciências Biológicas, Universidade Federal de Minas Gerais (UFMG), Belo Horizonte, Minas Gerais, Brazil.
[8]Laboratório de Flavivírus, Instituto Oswaldo Cruz, Fundação Oswaldo Cruz, Rio de Janeiro, Brazil.

Corresponding Author:
Bruno Silva Andrade
Av. José Moreira Sobrinho, s/n - Jequiezinho, Jequié, Bahia, 45205-490, Brazil
Email address: bandrade@uesb.edu.br

Abstract

Background: SARS-CoV-2 that are the causal agent of a current pandemic are enveloped, positive-sense, single-stranded RNA viruses of the Coronaviridae family. Proteases of SARS-CoV-2 are necessary for viral replication, structural assembly and pathogenicity. The ~33.8KDa M^{pro} protease of SARS-CoV-2 is a non-human homologue and highly conserved among several coronaviruses indicating M^{pro} could be a potential drug target for Coronaviruses.
Methods: Here we performed computational ligand screening of four pharmacophores (OEW, Remdesivir, Hydroxycholoquine and N3) that are presumed to have positive effects against

Preprints (www.preprints.org) | NOT PEER-REVIEWED | Posted: 1 April 2020 doi:10.20944/preprints202004.0003.v1

SARS-CoV-2 M^{pro} protease (6LU7) and also screened 50,000 molecules from the ZINC Database dataset against this protease target.
Results: We found 40 pharmacophore-like structures of natural compounds from diverse chemical classes that exhibited better affinity of docking as compared to the known ligands. The 10 best selected ligands namely, ZINC1845382, ZINC1875405, ZINC2092396, ZINC2104424, ZINC44018332, ZINC2101723, ZINC2094526, ZINC2094304, ZINC2104482, ZINC3984030, and ZINC1531664, are mainly classified as β-carboline, Alkaloids and Polyflavonoids, and all of them displayed interactions with dyad CYS145 and HIS41 from the protease pocket in a similar way as with other known ligands.
Conclusion: Our results suggest that these 10 molecules could be effective against SARS-CoV-2 protease and may be tested *in vitro* and *in vivo* to develop novel drugs against this virus.

Keywords: SARS-CoV-2, protease, virtual screening, pharmacophore, inhibitors, natural compounds

Introduction

Coronaviruses (CoVs) are enveloped, positive-sense, single-stranded RNA viruses of the Coronaviridae family (Cui et al., 2019). Based on their antigenic properties, they were classified into three main groups (Schoeman and Fielding, 2019): i) alpha-CoVs, responsible for gastrointestinal disorders; ii) beta-CoVs, which includes: (a) Bat coronavirus (BCoV), (b) the human Severe Acute Respiratory Syndrome (SARS) virus, (c) Middle Eastern Respiratory Syndrome (MERS) virus; and iii) gamma-CoVs, that mainly infect avian species. The most well-known of these coronaviruses is the SARS-CoV ("severe acute respiratory syndrome"), responsible for causing an outbreak in 2002-2003 (Peiris et al., 2004) and MERS-CoV ("Middle East respiratory syndrome"), causing severe respiratory symptoms, that was identified in 2012 (Zaki et al., 2012).

In December 2019, a series of unusual pneumonia cases caused by a novel coronavirus, recently renamed as severe acute respiratory syndrome coronavirus 2 (SARS-CoV-2), was identified in Wuhan (China) (Benvenuto, et al., 2020; Wu et al., 2020). The disease caused by SARS-CoV-2 is now

Preprints (www.preprints.org) | NOT PEER-REVIEWED | Posted: 1 April 2020 doi:10.20944/preprints202004.0003.v1

called COVID-19, and presents vast pathophysiological aspects, which include symptoms such as fever and coughing and up to severe acute respiratory failure (Zheng, 2020).

Since the infection crossed geographical barriers, the World Health Organization (WHO) declared a pandemic situation in March 2020, reaching a worldwide mortality rate of approximately 3% (Zhang, et al., 2020).

The SARS-CoV-2 virus genome has 15 ORFs: ORF 1a (encoded nonstructural proteins - nsp1 to nsp11), ORF 1b (encoded nonstructural proteins (nsp12 to nsp16), ORF S (encoded a Spike protein, binding to cell receptor and mediate virus-cell fusion), ORF 3a, 3b, 6, 7a, 7b, 8, 9a, 9b and 10 (encoded accessory protein), ORF E (encoded envelope protein, virus assembly and morphogenesis proteins), ORF M (encoded membrane protein and virus assembly proteins) and ORF N (encoded nucleocapsid protein, exhibits complex forms with genomic RNA, and interacts with M protein for viral assembly) (Wu et al., 2020).

ORF 1ab is a characteristic of members of the Coronaviridae family (Cheng et al., 2007) and is equivalent to two-thirds of the SARS-CoV-2 virus genome (Guo et al., 2019). Each of these ORFs, encodes a polyprotein (pp), which, when cleaved by proteases contained in the sequence, will generate 11 proteins (pp 1a) and 5 proteins (pp 1ab). The functions associated with these proteins are related to the virus replication processes, and the modulation of the immune response in the host, among other essential functions for the development of the pathogen within the host cell (Wu et al., 2020).

Preprints (www.preprints.org) | NOT PEER-REVIEWED | Posted: 1 April 2020 doi:10.20944/preprints202004.0003.v1

Virus resistance to drugs can lead to the emergence of new epidemics, such as Influenza A virus (IAV), and resistance to drugs with adamantanes and neuraminidase end up generating new outbreaks of the disease (Hussain et al., 2017). Both drugs act by inhibiting proteins that are located in the viral envelope, and this region is in greater contact with the external environment, suffering greater evolutionary pressure and consequently mutations. Drug resistance can occur when rapid viral replication is not repressed to the maximum (McKeegan et al., 2002). In contrast, virus proteases play a crucial role during virus replication, being a great target for drug discovery (Sharma and Gupta, 2017).

For viral replication, proteases are necessary for the assembly of the viral structure, and has been suggested to have relationships with the mechanism of infection and pathogenicity of SARS-CoV-2 (Zhang, et al., 2020; Benvenuto, et al., 2020). Proteases are enzymes found in all living organisms and viruses and are classified according to their catalytic nature. Proteases are divided into seven groups: aspartic proteases, asparagine peptide lyase, cysteine proteases, glutamic proteases, metalloproteases, serine proteases, and threonine proteases. Different types of proteases can perform the same activity through different catalytic mechanisms (Sharma and Gupta, 2017). A protease commonly has a binding site and a catalytic site that are very close in the protein structure (Sharma and Gupta, 2017). Proteases are present in several types of viruses and are widely found in human viruses (Patel, 2017).

In coronaviruses, pp1 (poly protein 1) is essential for the replication of the virus, as it encodes the protease M^{pro}, which is also called the "main protease" (Anand et al., 2002; Jin et al., 2020). M^{pro} is classified as a

Preprints (www.preprints.org) | NOT PEER-REVIEWED | Posted: 1 April 2020 doi:10.20944/preprints202004.0003.v1

chymotrypsin-like cysteine protease (3CLpro) (Anand et al., 2002; Bzowka et al., 2020), and the M^{pro} protease of SARS-CoV-2 with mass ~33.8KDa (JIN et al., 2020) is characterized by a self-cleavage protein (Cui et al., 2019; Kannan et al., 2020). It consists of a homodimer subdivided into two protomers (A and B) that have three distinct domains (Yang, et al., 2020). The first and second domains have antiparallel structure of β sheets while the third domain contains five α helices forming a globular group, which is connected in parallel with the domain-II through a loop region (Jin et al., 2020). The M^{pro} of SARS-CoV-2 has a catalytic cleft, comprising of a Cys-His dyad in the place of the protease substrate interaction, which is situated between domains -I and -II (Jin et al., 2020). It has non-canonic specificity to the substrate in the C-terminal portion. Furthermore, there is no homologue of M^{pro} in the human genome (Zheng, et al., 2020; Jin, et al., 2020), and it is highly conserved amongst coronaviruses (Xu et al., 2020). Therefore, M^{pro} is a potential target for studying inhibitors.

Antiviral therapy considers three main approaches to control and avoid viral infections: (a) vaccination, (b) stimulation of host resistance mechanisms, and (c) antiviral chemotherapy. Antivirals are drugs that inhibit certain virus-specific events, such as binding to host cells, which is how SARS-Cov-2 binds to ACE2 and TMPRSS2 (Hoffamann et al., 2020), and MERS binds to the DPP415 receptor (Zumla et al., 2016), stripping off the viral genome or clustering the progeny virions or preferably blocking the synthesis of virus-driven macromolecules (Agrawal et al., 2015). Antiviral chemotherapy can involve interfering with any or all of these virus replication steps. Most antiviral drugs are primarily targeted to the synthesis of nucleic acids in viruses. As viral replication and host cell

Preprints (www.preprints.org) | NOT PEER-REVIEWED | Posted: 1 April 2020 doi:10.20944/preprints202004.0003.v1

processes are closely linked, one of the main problems of viral therapy would be to find a drug capable of being selectively toxic just for the virus. Antivirals are frequently more effective in prevention than in the treatment itself, and are ineffective in eliminating latent or non-replicating viruses (Crumpacker, 2004). In addition, when selecting an antiviral drug, viral resistance must also be considered since it is one of the main causes of therapeutic failure.

The main classes of antiviral drugs used in clinical therapy to treat systemic viral infections include: a) Synthetic nucleosides (acyclovir, famciclovir, ganciclovir, valacyclovir, and valganciclovir; b) Pyrophosphate analogs (foscarnet); c) drugs for syncytial virus and influenza A (amantadine and rimantadine hydrochloride and ribavirin); d) Nucleoside reverse transcriptase inhibitors (NRTI: abacavir, didanosine, emtricitabine, stavudine, lamivudine, zidovudine, tenofovir in combination with NRTI); e) Non-nucleoside reverse transcriptase inhibitors (NNRTI: delavirdine, efavirenz, nevirapine); and f) Protease inhibitors (amprenavir, atazanavir, darunavir, fosamprenavir, lopinavir and ritonavir, nelfinavir mesylate, saquinavir mesylate, ritonavir, indinavir sulfate and tipranavir) (Ter et al., 2010; Larson et al., 2016; Balayan et al., 2017).

The study of inhibitors to reduce viral replication can bring short-term results, besides also reducing the severity and spread of the disease. Moreover, the use of antiviral compounds can assist in the prophylaxis of SARS-CoV-2 and reduce its spread (Mitjà and Clotet, 2020). Therefore, screening for potential viral protease inhibitors may assist in the selection of new drugs with antiviral potential for SARS-CoV-2.

Materials & Methods

Preprints (www.preprints.org) | NOT PEER-REVIEWED | Posted: 1 April 2020 doi:10.20944/preprints202004.0003.v1

Virtual screening

We used the crystallographic structure of COVID-19 main protease M^{pro} (6LU7) complexed with a known inhibitor, N3, for virtual screening (6Y7M) (Jin, et al., 2020). Both ligand based (LBVS) and receptor based virtual screening (RBVS), considering 50.000 structures of natural compounds from ZINC Database (https://zinc15.docking.org/) (Sterling and Irwin, 2015) were employed. ZINC molecules were downloaded that were restricted to ADMET characteristics for druglikeness: no more than 5 hydrogen bond donors, no more than 10 hydrogen bond acceptors, molecular weight between 160 and 500 g/Mol and logP between -0.4 and 5.6 (Guan et al., 2018; Lipinski et al., 2001; Ghose et al., 1999). For LBVS, we defined four known drugs divided in the following groups: 1) crystallographic (N3 and OEW), anti-viral (Remdesivir) and investigational (hydroxychloroquine), for chemical comparison with our database. We used a simple run with vROCS (OpenEye) (Hawkins et al., 2007) for generating queries with the pharmacophoric map with the stereochemical characteristics for each known ligand. Afterwards, we submitted each ligand query for searching similar pharmacophore-like molecules using Tanimoto Combo algorithm (Rácz et al., 2018; Bajusz et al., 2015) with 1.0 cutoff, which returned the best 1.000 hits for each round. This procedure was repeated three times for each query, and, subsequently, redundant structures were discarded, generating, in the end, a total of 4.000 similar molecules for docking experiment.

The best LBVS hits were submitted to molecular docking calculations with the COVD-19 main protease (6LU7) using Autodock 4.2 virtual screening protocol (Morris et al., 2009). All the ligand molecules and 6LU7 structure

Preprints (www.preprints.org) | NOT PEER-REVIEWED | Posted: 1 April 2020 doi:10.20944/preprints202004.0003.v1

were converted to its correspondent pdbqt files, using Autodock Tools 1.5.6 (Morris et al., 2009). The gridbox was defined on the active site region, considering the amino acids THR 190, GLU 166, GLN 189, GLY 143, HIS 163, HIS 164, CYS 145, PHE 140, and according to previous studies with the crystallographic structure of SARS-CoV-2 main protease (Wang et al., 2020; Zhang et al., 2020; Jin et al., 2020). Each docking run was performed three times using the following specifications: flexible docking and Lamarckian Genetic Algorithm with 1750000 generations. Afterwards, the 10 best docking hits were selected based on the average of affinity energy values, and classified according to their pharmacophore similarity. Additionally, we evaluated each docking position inside the 6LU7 active site using Pymol 2.1 (Schrödinger, 2020) in order to confirm molecule interactions with the amino acids within the protease active site. Furthermore, 2D interaction maps were generated by Discovery Studio 2019 (Dassault Systèmes BIOVIA, 2019).

Results

Ligand Based Virtual Screening (LBVS)

Different pharmacophoric characteristics were generated for each known ligand **(Figure 1)**, which allowed us to find molecules included in different chemical classifications and amplifying the number of possible drug candidates. **Table 1** shows the pharmacophoric characteristics for each known 6LU7 inhibitor, which allowed us to find natural ligands with pharmacophore-like regions. Additionally, we used the ADMET characteristics for molecular weight and LogP that are important for molecular druggability.

Preprints (www.preprints.org) | NOT PEER-REVIEWED | Posted: 1 April 2020 doi:10.20944/preprints202004.0003.v1

Ligand based virtual screening and docking calculations of ZINC database compounds revealed the 40 best pharmacophore-like ligands that belong to different chemical classes, namely, β-carboline Alkaloids, Indole Alkaloids, Lupin Alkaloids, Harmala Alkaloids, Polyflavonoids, Anthracenes, Angular Pyranocoumarins, and Flavonoid-3-O-glycosides. **Table 2** shows the detailed results on the average affinity energies, ZINC identification, and chemical classification of each selected ligand.

For selecting the best pharmacophore-like drug-candidates, we considered evaluating lower affinity energy values, as well as interactions with residues of the active site within the target. As can be seen in **figure 2A**, all pharmacophore-like OEW ligand molecules formed a complex with the active pocket of 6LU7. The three best OEW ligands (ZINC1845382, ZINC1875405, ZINC2092396) are shown in complex with COVID-19 protease in **Figure 2 (B to D)** with the detailed 2D interaction map. In this case, these top three hits are included in the -carboline alkaloid class.

The intermolecular interactions carried out by **ligand ZINC1845382** exhibited a hydrogen bond with the residue of the active PHE140 protease site. The catalytic residues CYS145 and HIS41 performed interactions of the type π, π-π stacked and π-alkyl with the entire beta-carboline group, which was composed of three hydrophobic rings. The remaining residues were of the π-sigma type, hydrogen-carbon acceptors, and halogen acceptors from residues THR25, THR26, as well as other residues from the active site GLU166, GLN189, GLY143, HYS164, respectively.

Ligand ZINC1875405 performed two hydrogen bonding interactions with residues THR25 and PHE140. Additionally, four more polar interactions of the type π-π stacked, π-aquil, aquil and π-sulfur with residues HIS41,

Preprints (www.preprints.org) | NOT PEER-REVIEWED | Posted: 1 April 2020 doi:10.20944/preprints202004.0003.v1

MET49, CYS145 and MET165, respectively, were formed. The other interactions were of hydrophobic van der Waals type.

Ligand **ZINC2092396** interacted by hydrogen interaction with the residue PHE140, π and π-alkyl with CYS140, π-π stacked and π-alkyl HIS41, and van der Waals with GLN189, GLY143, HIS164, GLU166. Other interactions occurred with hydrogen bonds by the ligand nitrobenzene group with the ASN142 residue and a π-sulfur interaction of the beta-carboline group with MET165 residue.

The Remdesivir pharmacophore-like search returned two Beta-carboline alkaloids **ZINC2104424** and **ZINC1875405**, as well as one polyflavonoid (**ZINC44018332**), which interacted with the COVID-19 main protease active pocket showing affinity energies below -10.0 Kcal/Mol. **Figure 3 (A to D)** show the details of all ligand interactions, as well as the top three molecules interaction maps.

The **ligand ZINC2104424** also occupied the region of the active site (**Figure 3 B**), showing polar interactions π, π-alkyl, π-π stacked and π-sulfur types from beta-carboline with HIS41, MET49, CYS145, and MET165 amino acids. Moreover, an interaction of THR26 halogen with the ligand Fluorobenzene group also occurred. Other hydrophobic interactions were van der Waals, mostly with residues of the active site: PHE140, GLY143, HIS163, HIS164, GLU166 and GLN189.

Ligand ZINC1875405 (Figure 3 C) displayed three hydrogen interactions with the indole group, and two oxygen interactions from a nitrobenzene of THR25, PHE140 AND GLN166, respectively. Several van der Waals-type hydrophobic interactions were found with GLY143, HIS164 and GLN189 amino acids. Furthermore, four polar interactions (π, π-alkyl, π-π stacked

Preprints (www.preprints.org) | NOT PEER-REVIEWED | Posted: 1 April 2020 doi:10.20944/preprints202004.0003.v1

and π-sulfur) with residues HIS41, MET49, CYS 145 and MET165, respectively, were also retrieved.

Ligand ZINC2092396 (Figure 3 D) exhibited two hydrogen interactions with HIS163 and THR26 by its hydroxyl from the flavonoid nucleus, as well as four more π-donor hydrogen bonding interactions with residues TYR54, PHE140, GLY143 and GLU166. Besides, three π-alkyl and π-sulfur interactions made with MET49, CYS145 and MET165 were also retrieved. Other hydrophobic interactions were of van der Waals type.

Figure 4 explains the interactions between 6LU7 active sites and the three best hits from derived molecules of hydroxychloroquine pharmacophore (ZINC2101723, ZINC2094526, ZINC2094304). These complexes displayed affinity energies varying from -10.2 Kcal/Mol to -9.6 Kcal/Mol, and all ligands were classified as -carboline alkaloids derivatives.

The beta-carboline group of the **ligand ZINC2101723** (**Figure 4 B**) formed four π-alkyl, alkyl and π-sulfur type interactions with HIS41, MET49, CYS145 and MET165 residues, as well as other hydrophobic interactions from its naphthalene and beta-carboline groups with the active site amino acids PHE140, GLY143, HIS163 E 164, GLU166 and GLN189. **Ligand ZINC2094526** (**Figure 4 C**) displayed a hydrogen bond interaction with PHE140 by its nitrobenzene group. Five polar interactions (π-sigma, π-aquil, π-π stacked and π-sulfur) were observed with residues THR25, HIS41, MET49, CYS145 and MET165, respectively. For the **ligand ZINC2094304** (**Figure 4 D**), two hydrogen bonds with residues PHE140 and GLU166 by its nitrobenzene group were formed. In addition, this ligand formed four polar interactions (π-π stacked, π-alkyl, alkyl and π-

Preprints (www.preprints.org) | NOT PEER-REVIEWED | Posted: 1 April 2020 doi:10.20944/preprints202004.0003.v1

sulfur) with residues HIS41, MET49, CYS145 and MET165, respectively. Other van der Waals type interactions could also be identified.

The N3 pharmacophore revealed one -carboline alkaloid (ZINC2101723) and two polyflavonoids (ZINC2094526 and ZINC2094304). This group displayed affinity energies ranging from -9.8 Kcal/Mol to -10.1 Kcal/Mol. **In figure 5** the best complex interactions with the protease, as well as their positions inside the binding pocket are depicted.

Ligand ZINC2104482 (**Figure 5 B**) formed a large number of hydrophobic interactions (14 van der Waals interactions), surrounding the active site amino acid, such as GLY143, HIS164, GLU166 and GLN189. Furthermore, this ligand formed three π-alkyl and alkyl bonds with HIS41, MET49, CYS145 residues. **Ligand ZINC3984030** (**Figure 5 C**) exhibited three hydrogen bonds with THR26, TYR54 and GLU166 residues by OH groups of flavonoid nuclei. A π-donor hydrogen bond interaction of the GLY143 residue was also observed. Moreover, three polar interactions (π-π stacked, π-alkyl and π-sulfur) were identified with HIS41, CYS145 and MET165. The rest of the interactions were van der Waals type. **Ligand ZINC1531664** (**Figure 5 D**) showed a hydrogen bond by its OH group TYR54. In addition, four π-donor hydrogen bond and hydrogen carbon bond interactions with residues PHE140, GLY143, GLU166 also occurred. Two polar interactions of the type π-alkyl and π-sulfur were observed with MET49, CYS145 and MET165, and the other hydrophobic interactions were of van der Waals type.

Discussion

Docking results revealed 40 pharmacophore-like natural ligands, which can be used as drug candidates for inhibiting SARS-CoV-2 main protease

 doi:10.20944/preprints202004.0003.v1

activity. Furthermore, we ranked the three best candidates for each known ligand pharmacophore as the best potential drug molecules (and totaling 12 molecules) for *in vitro* and *vivo assays* purposes, but not excluding the other 28 molecules. For these cases, ligands are included in two most expressive chemical classes: β-carboline Alkaloids and Polyflavonoids. Additionally, all ligands exhibited better affinity energies than the known drugs used as references for construction of pharmacophoric characteristics: OEW (Zhang et al., 2020), Remdesivir (Martinez, 2020), Hydroxychloroquine (Vincent et al., 2005), and N3 (Jin et al., 2020).

The groups of OEW and hydroxychloroquine pharmacophores presented their three most promising ligands classified as β-carboline Alkaloids. This class of molecules is reported by different authors with antiviral activities. According to Gonzalez et al. (2018), β-carboline Alkaloids are widely distributed in nature, and its derivatives exhibited activity against Herpes Simplex Viruses by blocking virus replication. Additionally, Gonzalez et al. (2018) demonstrated the action of these alkaloids in Dengue Virus (DENV-2) RNA replication. Furthermore, several other studies suggest the alkaloid activity against viral proteases (Ahmad et al., 2008; ul Qamar et al., 2014; Powers and Setzer, 2016). Similarly, Remdesivir pharmacophore revealed two β-carboline Alkaloids (ZINC2104424 and ZINC1875405), In addition, we detected a polyflavonoid (ZINC44018332) as one probable active molecule from a different class against SARS-CoV-2 main protease, and, several authors have described flavonoid activity as viral protease inhibitors (Qamar et al., 2017; Shimizu et al., 2017; Hawas et al., 2019), as well as antiviral molecules acting in different target classes (Kaul et al., 1985; Shimizu et al., 2017; González-Búrquez et al., 2018; Dai et al.,

Preprints (www.preprints.org) | NOT PEER-REVIEWED | Posted: 1 April 2020 doi:10.20944/preprints202004.0003.v1

2019). N3 pharmacophore displayed two flavonoids as the best molecules and just one β-carboline alkaloid. These results indicate that both classes of molecules could be explored for *in vitro* and *in vivo* tests to evaluate their potential antiviral activities for not only SARS-CoV-2 but also other viruses of medical interest.

Other classes of molecules were found in our screening for protease activity that were previously described in antiviral studies: Anthracenes (Tomlinson et al. 2011), Angular Pyranocoumarin (Barnard et al., 2002; Hassan et al., 2016), and Flavonoid-3-O-glycoside (Behbahani et al., 2014). Interaction maps of these complexes can be verified in the Supplementary Material.

All the known ligands (OEW, Remdesivir, Hydroxychloroquine and N3), that were used for validating our computational screening, exhibited worse affinity energies in docking calculations (ranging from -7.8 Kcal/Mol to -5.2 Kcal/Mol) than the natural screened compounds (ranging from -10.6 Kcal/Mol to -9.1 Kcal/Mol). Moreover, all the 40 selected ligands docked inside M^{pro} active site as previously described in several antiviral studies, and interacted in the region of connection between domains I and II with amino acids HIS41 and CYS145 (Zhang et al., 2020; Jin et al., 2020; Ren et al., 2013; Wang et al., 2016; Yang et al., 2003; Anand et al., 2002).

Zhang et al. (2020) studied four M^{pro} ketoamide inhibitors, including the OEW ligand (ligand 13b) used in our study, and detected a reduction in RNA replication in human cells infected with SARS-CoV-2, as well as described binding interactions with its main protease. Besides, they propose a ketoamide as a probable protease inhibitor and a drug candidate against the virus.

Preprints (www.preprints.org) | NOT PEER-REVIEWED | Posted: 1 April 2020 doi:10.20944/preprints202004.0003.v1

The peptidomimetic molecule N3 was proposed as a drug candidate by Wang and colleagues (2020), describing its binding interactions with the crystallographic structures of SARS-CoV-2 and other viral proteases. Their study reported that N3 can bind in all active pockets from the main proteases of HCoV-NL63, SARS-CoV, and MERS-CoV.

Other molecules have been tested as antivirals for effectiveness in inhibiting SARS-CoV-2 replication in cell culture. Two drugs exhibited a promising inhibitory effect: remdesivir (GS-5734), an experimental drug being developed for the treatment of Ebola virus infection (Warren et al., 2016); and hydroxychloroquine (CQ), a drug known for its effectiveness in the treatment of malaria and autoimmune diseases (Wang et al., 2020). The Remdesivir, or GS-5734, is an adenosine triphosphate analogue initially described in the literature in 2016 as a potential treatment for Ebola (Warren et al., 2016), and this drug has been indeed considered as a potential treatment for SARS-CoV2, (De Wit et al., 2020). Notably, remdesivir has demonstrated antiviral activity in the treatment of MERS and SARS in animal models, both of which are caused by the coronavirus (Sheahan et al., 2017). Hydroxychloroquine is an aminoquinoline-like chloroquine (Furst, 1996). It is a drug commonly prescribed for the treatment of uncomplicated malaria, rheumatoid arthritis, chronic discoid lupus erythematosus, and systemic lupus erythematosus (Shippey et al., 2018). Chloroquine and hydroxychloroquine are being investigated for the treatment of SARS-CoV-2 (Devaux et al., 2020), and they have been reported to have direct antiviral effects, such as inhibition of flaviviruses, retroviruses (like HIV), and many coronaviruses. A recent study showed that, with EC50 of 1.13 μmol / L and SI greater than 88, chloroquine can

 doi:10.20944/preprints202004.0003.v1

effectively inhibit SARS-CoV-2 at the cellular level. Its effectiveness in the human body for SARS-CoV-2 infection however, has not yet been clinically proven. Carong et al. (2020) carried out an *in silico* study with chloroquine and detected interactions with viral Nsp3b type protease.

Conclusions

In our study, we compared the pharmacophores of four well-tested Human-CoV (and including SARS-Cov-2) main protease drug candidates to 50,000 structures of natural compounds from the ZINC Database. The three best molecules selected for each pharmacophore class are mainly classified as β-carboline alkaloids, and polyflavonoids. The best ligand-SARS-Cov-2 complexes exhibited better affinity energies in comparison to drug molecules used in this study. Furthermore, all the screened molecules bonded between domains -I and -II and formed interactions with the catalytic residues HIS41 and CYS145 in similar positions as previously described from other authors in viral protease inhibitor studies. Altogether, we propose these compounds as possible SARS-CoV-2 protease inhibitors, which can be used for *in vitro* and *in vivo* tests for finding novel drug candidates.

Acknowledgements

We would like to thank The OpenEye Science for the OpenEye Software license, which made possible the ligand based virtual screening experiments.

References

Agrawal AS, Garron T, Tao X, Peng BH, Wakamiya M, Chan TS, Couch RB, Tseng CT. 2015. Generation of a transgenic mouse model of Middle East

respiratory syndrome coronavirus infection and disease. *Journal of Virology* 89:3659-70 DOI: 10.1128/JVI.03427-14.

Ahmad I, Fatima I, Afza N, Malik A, Lodhi MA, Choudhary MI. 2008. Urease and serine protease inhibitory alkaloids from Isatis tinctoria. *Journal of Enzyme Inhibition and Medicinal Chemistry* 23(6):918-21 DOI: 10.1080/14756360701743580.

Anand K, Palm GJ, Mesters JR, Siddell SG, Ziebuhr J, Hilgenfeld R. 2002. Structure of coronavirus main proteinase reveals combination of a chymotrypsin fold with an extra alpha-helical domain. *The EMBO Journal* 21(13):3213-24. DOI: 10.1093/emboj/cdf327 DOI: 10.1093/emboj/cdf327.

Bajusz D, Rácz A, Héberger K. 2015. Why is Tanimoto index an appropriate choice for fingerprint-based similarity calculations? Journal of Cheminformatics 7:20. DOI: 10.1186/s13321-015-0069-3.

Balayan T, Horvath H, Rutherfor GW. 2017. Ritonavir-boosted darunavir plus two nucleoside reverse transcriptase inhibitors versus other regimens for initial antiretroviral Therapy for people with HIV infection: a Systematic review. *AIDS Research and Treatment* 2017:2345617. DOI: 10.1155/2017/2345617.

Barnard DL, Xu Ze, Stowell VD, Yuan H, Smee DF, Samy R, Sidwell RW, Nielsen MK, Sun L, Cao H, Li A, Quint C, Deignan J, Crabb J, Flavin MT. 2002. Coumarins and pyranocoumarins, potential novel pharmacophores for inhibition of measles virus replication. *Antiviral Chemistry & Chemotherapy* 13(1):39-59 DOI: 10.1177/095632020201300104.

Behbahani M, Sayedipour S, Pourazar A, Shanehsazzadeh M. 2014. In vitro anti-HIV-1 activities of kaempferol and kaempferol-7-O-glucoside isolated from Securigera securidaca. *Research in Pharmaceutical Sciences* 9(6):463-9.

Benvenuto D, Giovanetti M, Ciccozzi A, Spoto S, Angeletti S, Ciccozzi M. 2020. The 2019-new coronavirus epidemic: Evidence for virus evolution. *Journal of Medical Virology* 92(4):455-459 DOI: 10.1002/jmv.25688.

Bzówka M, Mitusińska K, Raczyńska A, Samol A, Tuszyński J, Góra A. 2020. Molecular Dynamics Simulations Indicate the COVID-19 Mpro Is Not a Viable Target for Small-Molecule Inhibitors Design. *bioRxiv* DOI:10.1101/2020.02.27.968008.

Cheng VC, Lau SK, Woo PC, Yuen KY. 2007. Severe acute respiratory syndrome coronavirus as an agent of emerging and reemerging infection. *Clinical microbiology reviews* 20(4):660-694 DOI: 10.1128/CMR.00023-07.

Crumpacker CS. 2004. Use of antiviral drugs to prevent herpes virus transmission. *New England Journal of Medicine* 350:67-68 DOI: 10.1056/NEJMe038189.

Cui J, Li F, Shi ZL. 2019. Origin and evolution of pathogenic coronaviruses. *Nature reviews Microbiology* 17(3):181-192 DOI: 10.1038/s41579-018-0118-9.

Dai W, Bi J, Li F, Wang S, Huang X, Meng X, Sun B, Wang D, Kong W, Jiang C, Su W. 2019. Antiviral Efficacy of Flavonoids against Enterovirus 71 Infection in Vitro and in Newborn Mice. *Viruses* 11(7):E625 DOI: 10.3390/v11070625.

Dassault Systèmes BIOVIA, [Discovery Studio Visualizer], [19], San Diego: Dassault Systèmes, [2019].

De Wit E, Feldmann F, Cronin J, Jordan R, Okumura A, Thomas T, Scott D, Cihlar T, Feldmann H. 2020. Prophylactic and therapeutic remdesivir (GS-5734) treatment in the rhesus macaque model of MERS-CoV infection. *Proceedings of the National Academy of Sciences of the United States of America* 117(12):6771-6776 DOI: 10.1073/pnas.1922083117.

Devaux CA, Rolain JM, Colson P, Raoult D. 2020. New insights on the antiviral effects of chloroquine against coronavirus: what to expect for

COVID-19? International Journal of Antimicrobial Agents DOI: 10.1016/j.ijantimicag.2020.105938.

Furst DE. 1996. Pharmacokinetics of hydroxychloroquine and chloroquine during treatment of rheumatic diseases. Lupus 5 (Suppl 1):S11-5.

Ghose AK, Viswanadhan VN, Wendoloski JJ. 1999. A knowledge-based approach in designing combinatorial or medicinal chemistry libraries for drug discovery. 1. A qualitative and quantitative characterization of known drug databases. ACS Combinatorial Science 1(1):55-68 DOI: 10.1021/cc9800071.

Gonzalez MM, Cabrerizo FM, Baiker A, Erra-Balsells R, Osterman A, Nitschko H,

González-Búrquez MJ, González-Díaz FR, García-Tovar CG, Carrillo-Miranda L, Soto-Zárate CI, Canales-Martínez MM, Penieres-Carrillo JG, Crúz-Sánchez TA, Fonseca-Coronado S. 2018. Comparison between In Vitro Antiviral Effect of Mexican Propolis and Three Commercial Flavonoids against Canine Distemper Virus. Evidence-based Complementary and Alternative Medicine 2018:7092416. doi: 10.1155/2018/7092416.

Guan L, Yang H, Cai Y, Sun L, Di P, Li W, Liu G, Tang Y. 2018. ADMET-score – a comprehensive scoring function for evaluation of chemical drug-likeness. Medchemcomm 10(1):148-157 DOI: 10.1039/c8md00472b.

Guo YR, Cao QD, Hong ZS, Tan YY, Chen SD, Jin HJ, Tan KS, Wang DY, Yan Y. 2020. The origin, transmission and clinical therapies on coronavirus disease 2019 (COVID-19) outbreak–an update on the status. Military Medical Research, 7(1):1-10 DOI: 10.1186/s40779-020-00240-0.

Harcourt BH, Jukneliene D, Kanjanahaluethai A, Bechill J, Severson KM, Smith CM, Rota PA, Baker SC. 2004. Identification of severe acute respiratory syndrome coronavirus replicase products and characterization of papain-like protease activity. Journal of virology 78(24):13600-13612 DOI: 10.1128/JVI.78.24.13600-13612.2004.

Hassan MZ, Osman H, Ali MA, Ahsan MJ. 2016. Therapeutic potential of coumarins as antiviral agents. *European Journal of Medicinal Chemistry* 123:236–255 DOI: 10.1016/j.ejmech.2016.07.056.

Hawas UW, Abou El-Kassem LT, Shaher F, Al-Farawati R. 2019. In vitro inhibition of Hepatitis C virus protease and antioxidant by flavonoid glycosides from the Saudi costal plant Sarcocornia fruticosa. *Natural Product Research* 33(23):3364–3371 DOI: 10.1080/14786419.2018.1477153.

Hawkins PCD, Skillman AG, Nicholls A. Comparison of Shape-Matching and Docking as Virtual Screening Tools. 2007. *Journal of Medicinal Chemistry* 50: 74–82 DOI: 10.1021/jm0603365.

Hoffmann M, Kleine-Weber H, Schroeder S, Krüger N, Herrler T, Erichsen S, Schiergens TS, Herrler G, Wu NH, Nitsche A, Müller MA, Drosten C, Pöhlmann S. 2020. SARS-CoV-2 Cell Entry Depends on ACE2 and TMPRSS2 and Is Blocked by a Clinically Proven Protease Inhibitor. *Cell* S0092-8674(20)30229-4 DOI: 10.1016/j.cell.2020.02.052.

Hussain M, Galvin HD, Haw TY, Nutsford AN, Husain M. Drug resistance in influenza a virus: The epidemiology and management. 2017. *Infection and Drug Resistance* 10:121–134 DOI: 10.2147/IDR.S105473.

Jin Z, Du X, Xu Y, Deng Y, Liu M, Zhao Y, Zhang B, Li X, Zhang L, Peng C, Duan Y, Yu J, Wang L, Yang F, Liu F, Jiang R, Yang X, You T, Liu X, Yang X, Bai F, Liu H, Liu X, Guddat LW, Xu W, Xiao G, Qin C, Shi Z, Jiang H, Rao Z, Yang H. 2020. Structure of Mpro from COVID-19 virus and discovery of its inhibitors (2020). *bioRxiv* DOI: 10.1101/2020.02.26.964882.

Kannan S, Shaik Syed Ali P, Sheeza A, Hemalatha K. 2020. COVID-19 (Novel Coronavirus 2019)–recent trends. *European Review for Medical and Pharmacological Sciences* 24:2006–2011 DOI: 10.26355/eurrev_202002_20378.

Kaul TN, Middleton E Jr, Ogra PL. 1985. Antiviral effect of flavonoids on human viruses. *Journal of Medical Virology* 15(1):71–9 DOI: 10.1002/jmv.1890150110.

Lipinski CA, Lombardo F, Dominy BW, Feeney PJ. 2001. Experimental and computational approaches to estimate solubility and permeability in drug discovery and development settings. *Advanced Drug Delivery Reviews* 46(1–3):3–26 DOI: 10.1016/s0169-409x(00)00129-0.

Martinez MA. 2020. Compounds with therapeutic potential against novel respiratory 2019 coronavirus. *Antimicrobial Agents and Chemotherapy* DOI: 10.1128/AAC.00399-20.

McKeegan KS, Borges-Walmsley MI, Walmsley AR. 2002. Microbial and viral drug resistance mechanisms. *Trends Microbiology* 10:8–14 DOI: 10.1016/S0966-842X(02)02429-0.

measures for interaction fingerprints. Journal of Cheminformatics 10(1):48 DOI: 10.1186/s13321-018-0302-y.

Mitjà O, Clotet B. 2020. Use of antiviral drugs to reduce COVID-19 transmission (2020). *The Lancet Global Health* DOI: 10.1016/S2214-109X(20)30114-5.

Morris, GM, Huey R, Lindstrom W, Sanner MF, Belew RK, Goodsell DS, Olson AJ. 2009. Autodock4 and AutoDockTools4: automated docking with selective receptor flexiblity. *Journal of Computational Chemistry* 16:2785–91 DOI: 10.1002/jcc.21256.

Muramatsu T, Takemoto C, Kim YT, Wang H, Nishii W, Terada T, Shirouzu M, Yokoyama S. 2016. SARS-CoV 3CL protease cleaves its C-terminal autoprocessing site by novel subsite cooperativity. *Proceedings of the National Academy of Sciences of the United States of America* 113(46):12997-13002 DOI: 10.1073/pnas.1601327113.

Patel, S. 2017. A critical review on serine protease: Key immune manipulator and pathology mediator. *Allergologia et Immunopathologia* 45(6):579–591 DOI: 10.1016/j.aller.2016.10.011.

Peiris JS, Guan Y, Yuen KY. 2004. Severe acute respiratory syndrome. *Nature Medicine* 10(12 Suppl):S88–97 DOI: 10.1038/nm1143.

Powers CN, Setzer WN. 2016. An In-Silico Investigation of Phytochemicals as Antiviral Agents Against Dengue Fever. *Combinatorial Chemistry & High Throughput Screening* 19(7):516–36 DOI: 10.2174/1386207319666160506123715.

Qamar MT, Ashfaq UA, Tusleem K, Mumtaz A, Tariq Q, Goheer A, Ahmed B. 2017. In-silico identification and evaluation of plant flavonoids as dengue NS2B/NS3 protease inhibitors using molecular docking and simulation approach. *Pakistan Journal of Pharmaceutical Sciences* 30(6):2119–2137.

Quintana VM, Piccini LE, Panozzo Zénere JD, Damonte EB, Ponce MA, Castilla V. 2016. Antiviral activity of natural and synthetic β-carbolines against dengue virus. *Antiviral Research* 134:26–33 DOI: 10.1016/j.antiviral.2016.08.018.

Rácz A, Bajusz D, Héberger K. 2018. Life beyond the Tanimoto coefficient: similarity

measures for interaction fingerprints. *Journal of Cheminformatics* 10(1):48 DOI: 10.1186/s13321-018-0302-y.

Ren Z, Yan L, Zhang N, Guo Y, Yang C, Lou Z, Rao Z. 2013. The newly emerged SARS-like coronavirus HCoV-EMC also has an "Achilles' heel": current effective inhibitor targeting a 3C-like protease. *Protein & Cell* 4(4):248–50 DOI: 10.1007/s13238-013-2841-3.

Schoeman D, Fielding BC. 2019. Coronavirus envelope protein: current knowledge. *Virology Journal* 16(1):69 DOI: 10.1186/s12985-019-1182-0.

Schrödinger, LLC. 2020. The PyMOL Molecular Graphics System, Version 2.0.

Seidah NG, Nichol ST. 2005. Chloroquine is a potent inhibitor of SARS coronavirus

Sharma A, Gupta SP. 2017. Viral Proteases and Their Inhibitors. In: Gupta SP, ed. *Fundamentals of viruses and their proteases.* Elsevier.

Sheahan TP, Sims AC, Graham RL, Menachery VD, Gralinski LE, Case JB, Leist SR, Pyrc K, Feng JY, Trantcheva I, Bannister R, Park Y, Babusis D, Clarke MO, Mackman RL, Spahn JE, Palmiotti CA, Siegel D, Ray AS, Cihlar T, Jordan R, Denison MR, Baric RS. 2017. Broad-spectrum antiviral GS-5734 inhibits both epidemic and zoonotic coronaviruses. *Science Translational Medicine* 28(9):396 DOI: 10.1126/scitranslmed.aal3653.

Shimizu JF, Lima CS, Pereira CM, Bittar C, Batista MN, Nazaré AC, Polaquini CR, Zothner C, Harris M, Rahal P, Regasini LO, Jardim ACG. 2017. Flavonoids from Pterogyne nitens Inhibit Hepatitis C Virus Entry. *Scientific Reports* 7(1):16127 DOI: 10.1038/s41598-017-16336-y.

Shippey EA, Wagler VD, Collamer AN. 2018. Hydroxychloroquine: An old drug with new relevance. *Cleveland Clinic Journal of Medicine* 85(6):459-467 DOI: 10.3949/ccjm.85a.17034.

Sterling T, Irwin JJ. 2015. ZINC 15--Ligand Discovery for Everyone. *Journal of Chemical Information and Modeling* 55(11):2324-37 DOI: 10.1021/acs.jcim.5b00559.

Ter Heine R, Muder JW, Van Gorp EC, Wagenaar JF, Beijnen JH, Huitema AD. 2020. Intracelular and plasma stead-state pharmacokinetics of raltegravir, darunavir, etravirine and ritonavir in heavily pre-treated HIV-infected patients. *British Journal of Clinical Pharmacology* 69:475-83 DOI: 10.1111/j.1365-2125.2010.03634.x.

Tomlinson SM, Watowich SJ. 2011. Anthracene-based inhibitors of dengue virus NS2B-NS3 protease. *Antiviral Research* 89(2):127-35 DOI: 10.1016/j.antiviral.2010.12.006.

ul Qamar M.T., Mumtaz A., Ashfaq U.A., Muzammal Adeel M., Fatima T. 2014. Potential of plant alkaloids as dengue ns3 protease inhibitors: Molecular docking and simulation approach. *Bangladesh Journal of Pharmacology* 9(3):262-267 DOI: 10.3329/bjp.v9i3.18555.

Vincent MJ, Bergeron E, Benjannet S, Erickson BR, Rollin PE, Ksiazek TG, Vizoso-Pinto MG. 2018. β-Carboline derivatives as novel antivirals for herpes simplex virus. *International Journal of Antimicrobial Agents* 52(4):459-468 DOI: 10.1016/j.ijantimicag.2018.06.019.

Wang F, Chen C, Tan W, Yang K, Yang H. 2016. Structure of Main Protease from Human Coronavirus NL63: Insights for Wide Spectrum Anti-Coronavirus Drug Design. *Scientific Reports* 6:22677 DOI: 10.1038/srep22677.

Wang Q, Qiu Y, Li JY, Zhou ZJ, Liao CH, Ge XY. 2020. A Unique Protease Cleavage Site Predicted in the Spike Protein of the Novel Pneumonia Coronavirus (2019-nCoV) Potentially Related to Viral Transmissibility. *Virology Sinica* DOI: 10.1007/s12250-020-00212-7.

Warren TK, Jordan R, Lo MK, Ray AS, Mackman RL, Soloveva V, Siegel D, Perron M, Bannister R, Hui HC, Larson N, Strickley R, Wells J, Stuthman KS, Van Tongeren SA, Garza NL, Donnelly G, Shurtleff AC, Retterer CJ, Gharaibeh D, Zamani R, Kenny T, Eaton BP, Grimes E, Welch LS, Gomba L, Wilhelmsen CL, Nichols DK, Nuss JE, Nagle ER, Kugelman JR, Palacios G, Doerffler E, Neville S, Carra E, Clarke MO, Zhang L, Lew W, Ross B, Wang Q, Chun K, Wolfe L, Babusis D, Park Y, Stray KM, Trancheva I, Feng JY, Barauskas O, Xu Y, Wong P, Braun MR, Flint M, McMullan LK, Chen SS, Fearns R, Swaminathan S, Mayers DL, Spiropoulou CF, Lee WA, Nichol ST, Cihlar T, Bavari S. 2016. Therapeutic efficacy of the small molecule GS-5734 against Ebola virus in rhesus monkeys. *Nature* 531(7594):381-5 DOI: 10.1038/nature17180

Wu F, Zhao S, Yu B, Chen YM, Wang W, Song ZG, Hu Y, Tao ZW, Tian JH, Pei YY, Yuan ML, Zhang YL, Dai FH, Liu Y, Wang QM, Zheng JJ, Xu L, Holmes EC, Zhang YZ. 2020. A new coronavirus associated with human respiratory disease in China. *Nature* 579(7798):265-269 DOI: 10.1038/s41586-020-2008-3.

Xu X, Chen P, Wang J, Feng J, Zhou H, Li X, Zhong W, Hao P. 2020. Evolution of the novel coronavirus from the ongoing Wuhan outbreak and modeling of its spike protein for risk of human transmission. *Science China Life Sciences* 63(3):457–460 DOI: 10.1007/s11427-020-1637-5.

Yang H, Yang M, Ding Y, Liu Y, Lou Z, Zhou Z, Sun L, Mo L, Ye S, Pang H, Gao GF, Anand K, Bartlam M, Hilgenfeld R, Rao Z. 2003. The crystal structures of severe acute respiratory syndrome virus main protease and its complex with an inhibitor. *Proceedings of the National Academy of Sciences of the United States of America* 100(23):13190–5 DOI: 10.1073/pnas.1835675100

Zaki AM, van Boheemen S, Bestebroer TM, Osterhaus AD, Fouchier RA. 2012. Isolation of a novel coronavirus from a man with pneumonia in Saudi Arabia. *New England Journal of Medicine* 367(19):1814–20 DOI: 10.1056/NEJMoa1211721.

Zhang L, Lin D, Sun X, Curth U, Drosten C, Sauerhering L, Becker S, Rox K, Hilgenfeld R. 2020. Crystal structure of SARS-CoV-2 main protease provides a basis for design of improved α-ketoamide inhibitors. *Science* DOI:10.1126/science.abb3405.

Zheng M, Gao Y, Wang G, Song G, Liu S, Sun D, Xu Y, Tian Z. 2020. Functional exhaustion of antiviral lymphocytes in COVID-19 patients. *Cellular & Molecular Immunology* DOI: 10.1038/s41423-020-0402-2.

Zumla A, Chan JF, Azhar EI, Hui DS, Yuen KY. 2016. Coronaviruses—drug discovery and therapeutic options. *Nature Reviews Drug Discovery* 15:327–47 DOI: 10.1038/nrd.2015.37.

Preprints (www.preprints.org) | NOT PEER-REVIEWED | Posted: 1 April 2020 doi:10.20944/preprints202004.0003.v1

Figure 1

Pharmacophore representation for each Known drug used for virtual screening.

A: OEW, **B**: N3, **C**: Remdesivir and **D**: Hydroxychloroquine. In red spheres: hydrogen acceptors; blue spheres: hydrogen donors; yellow spheres: hydrophobic; and green spheres: aromatic.

Preprints (www.preprints.org) | NOT PEER-REVIEWED | Posted: 1 April 2020 doi:10.20944/preprints202004.0003.v1

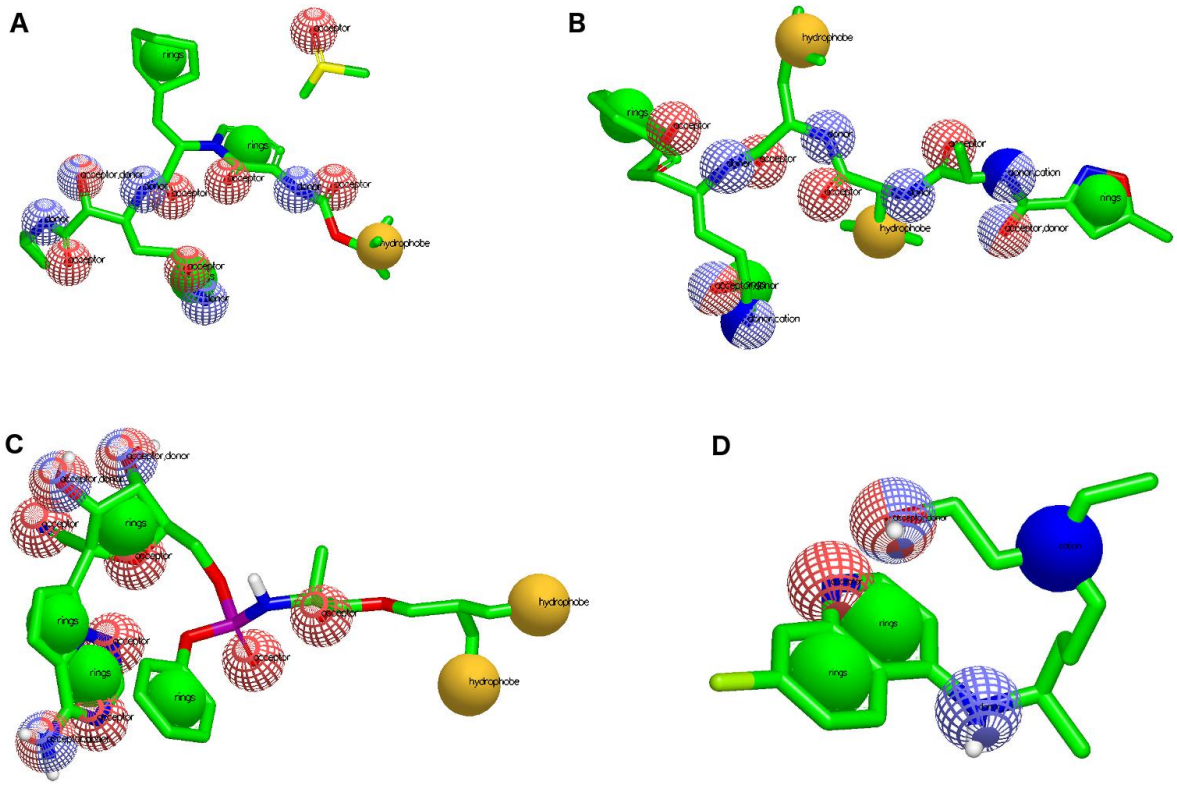

Figure 2

Best hits for OEW pharmacophore-like molecules

A: SARS-CoV-2 main protease complexed with the 10 best hits OEW pharmacophore molecules. Protomer A is represented in marine blue surface and

Preprints (www.preprints.org) | NOT PEER-REVIEWED | Posted: 1 April 2020 doi:10.20944/preprints202004.0003.v1

protomer B in dark pink surface. ZINC1845382 in cyan (B), ZINC1875405 (C) in dark pink and ZINC2092396 in purple (D) inside 6LU7 binding site and their 2D interaction maps with pocket amino acids.

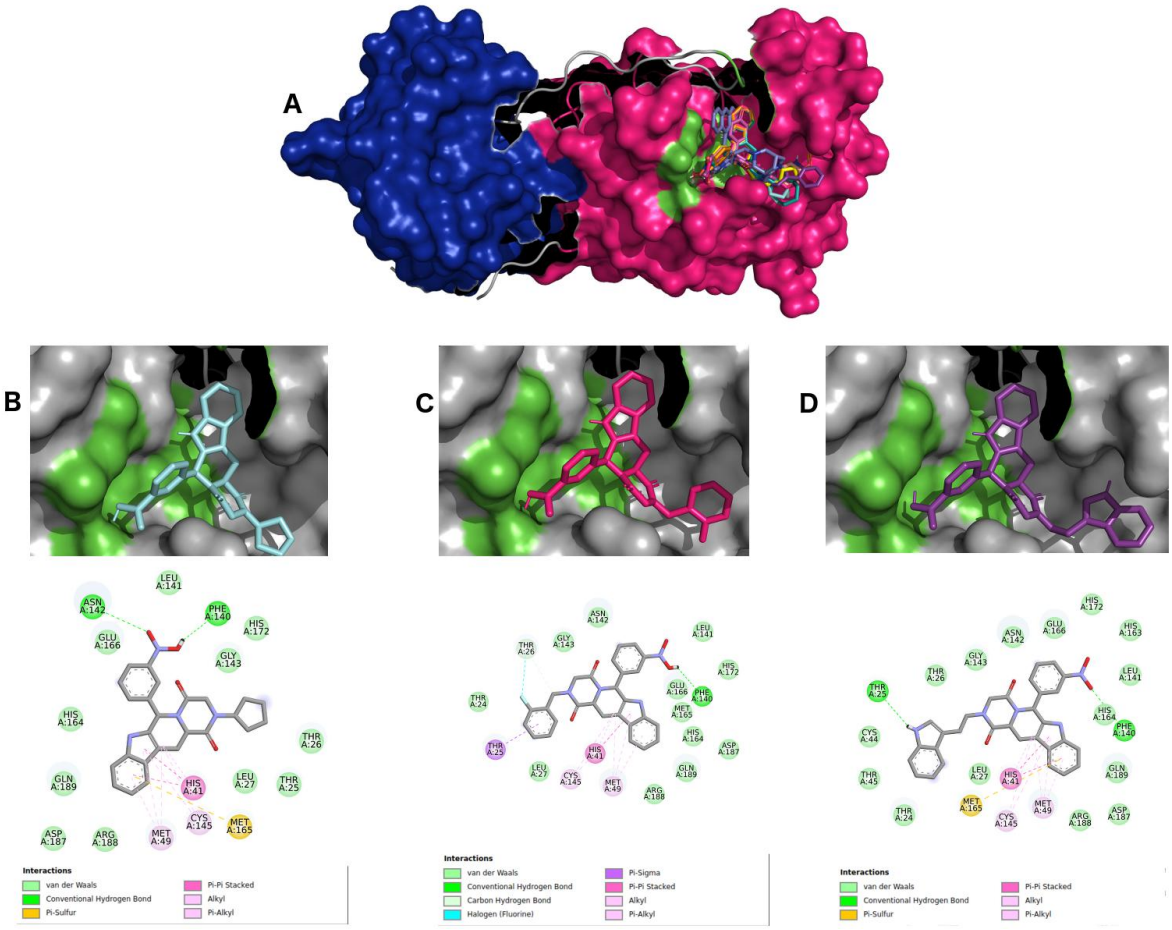

Figure 3

Preprints (www.preprints.org) | NOT PEER-REVIEWED | Posted: 1 April 2020 doi:10.20944/preprints202004.0003.v1

Best hits Remdesivir pharmacophore-like molecules

A: SARS-CoV-2 main protease complexed with 10 best hits Remdesivir pharmacophore molecules. Protomer A is represented in green surface, and protomer B in orange surface. ZINC2104424 in cyan (**B**), ZINC1875405 (**C**) in wheat and ZINC44018332 in violet (**D**) inside 6LU7 binding site and their 2D interaction maps with pocket amino acids.

Preprints (www.preprints.org) | NOT PEER-REVIEWED | Posted: 1 April 2020 doi:10.20944/preprints202004.0003.v1

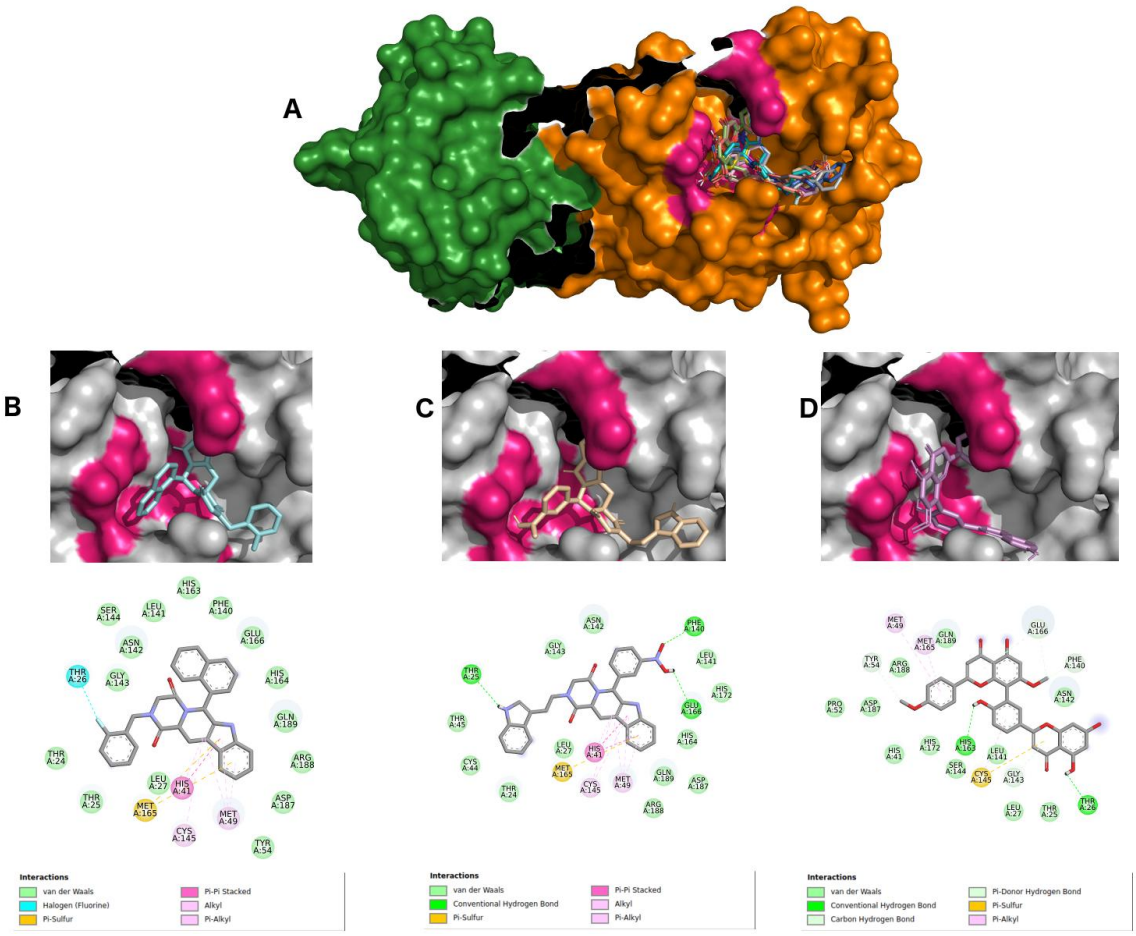

Figure 4

Best hits for Hydroxychloroquine pharmacophore-like molecules

A: Protomer A is represented in violet surface, and protomer B in marine blue surface. ZINC2101723 in

Preprints (www.preprints.org) | NOT PEER-REVIEWED | Posted: 1 April 2020 doi:10.20944/preprints202004.0003.v1

yellow (B), ZINC2094526 in red (C), and ZINC2094304 in dark blue (D) inside 6LU7 binding site and their 2D interaction maps with pocket amino acids.

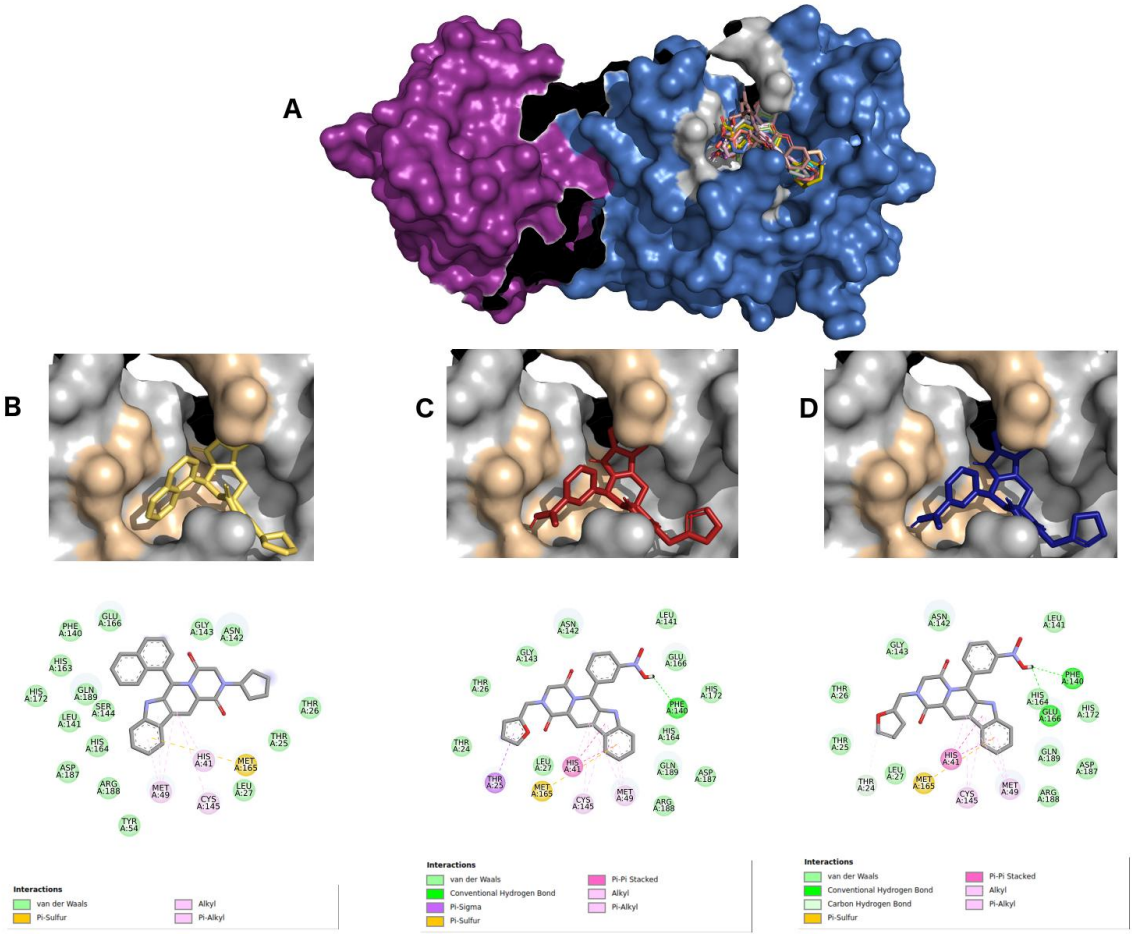

Figure 5

Preprints (www.preprints.org) | NOT PEER-REVIEWED | Posted: 1 April 2020 doi:10.20944/preprints202004.0003.v1

Virtual screening results for the N3 pharmacophore

A: SARS-CoV-2 main protease is represented in cyan (protomer A) and dark salmon (protomer B). The best complexes are formed by the alkaloid ZINC2101723 in pink (**B**) and two polyflavonoids ZINC2094526 in marine blue (**C**) and ZINC2094304 in lemon green (**D**), and their 2D interaction maps with pocket amino acids are shown below each complex.

Preprints (www.preprints.org) | NOT PEER-REVIEWED | Posted: 1 April 2020 doi:10.20944/preprints202004.0003.v1

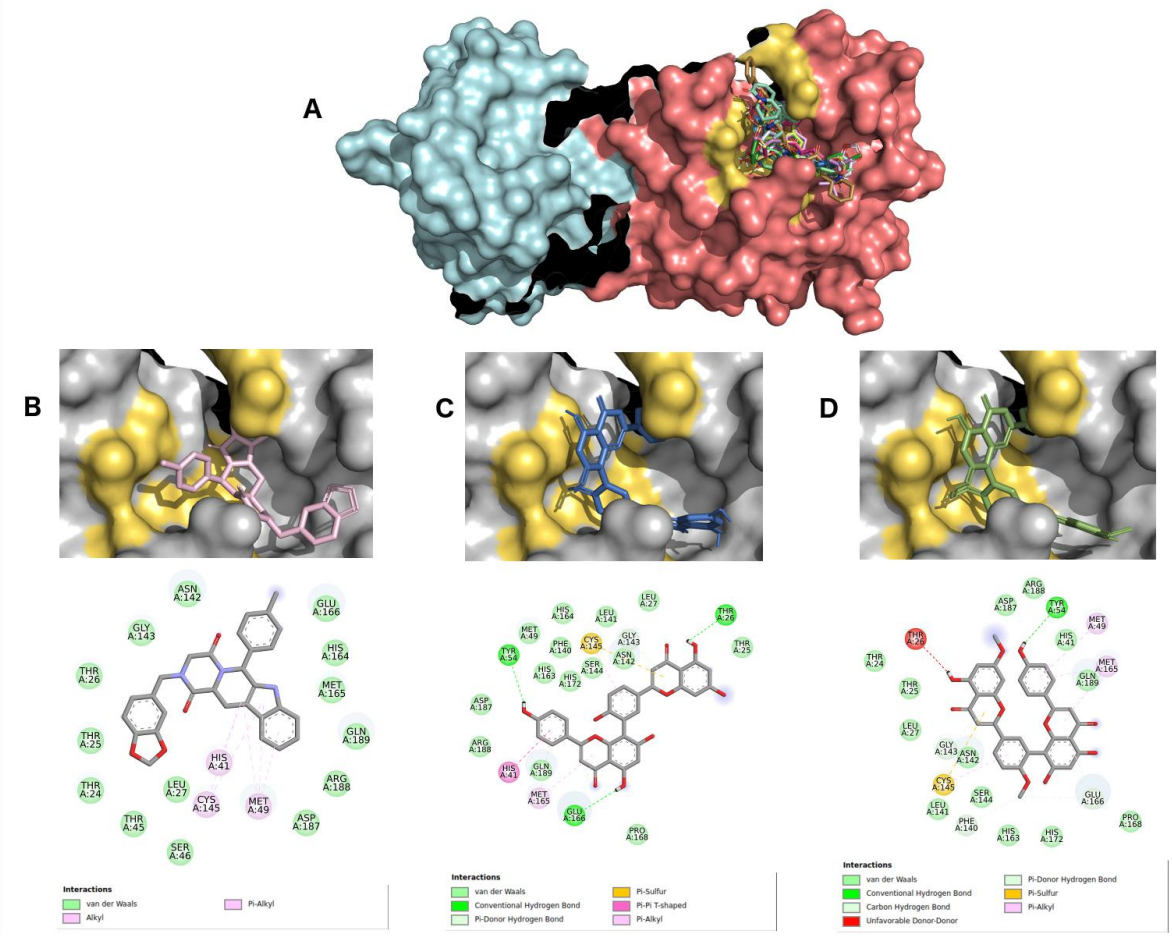

Table 1 (on next page)

Table1: Pharmacophoric characteristics for each known inhibitor used for screening natural ligands from ZINC Database **Hb.A.** = Hydrogen acceptor; **Hb.D.** = Hydrogen donor; **M.W.** = Molecular weight.

Preprints (www.preprints.org) | NOT PEER-REVIEWED | Posted: 1 April 2020 doi:10.20944/preprints202004.0003.v1

Inhibitor	Hb.A.	Hb.D.	Aromatic	Hydrophobic	M.W.	LogP
OEW	7	5	3	1	663.8	-0.71
N3	6	4	3	2	680.8	2.32
Remdesivir	9	1	4	2	602.6	1.9
Hydroxychloroquine	2	2	2	0	335.9	3.6

 doi:10.20944/preprints202004.0003.v1

 doi:10.20944/preprints202004.0003.v1

Table 2(on next page)

Table 2: 40 best molecule hits of SARS-CoV-2 main protease inhibitor candidates from a dataset of 50,000 natural compounds from ZINC Database

Preprints (www.preprints.org) | NOT PEER-REVIEWED | Posted: 1 April 2020 doi:10.20944/preprints202004.0003.v1

Known Drug	Ligand	Avg. Afinity (Kcal/Mol)	Classification
OEW (13b)	**OEW**	**-6.8**	**Ketoamide**
	ZINC1845382	-10.2	β-carboline Alkaloid
	ZINC1875405*	-10.1	β-carboline Alkaloid
	ZINC2092396	-9.8	β-carboline Alkaloid
	ZINC1900463	-9.8	β-carboline Alkaloid
	ZINC2149492	-9.8	β-carboline Alkaloid
	ZINC2112405	-9.7	β-carboline Alkaloid
	ZINC2095426	-9.7	β-carboline Alkaloid
	ZINC2094306	-9.6	β-carboline Alkaloid
	ZINC2144677	-9.6	Anthracene
	ZINC1095868	-9.5	Harmala Alkaloids
Remdesivir	**Remdesivir**	**-7.8**	**Peptide-like**
	ZINC2104424	-10.6	β-carboline Alkaloid
	ZINC1875405*	-10.1	β-carboline Alkaloid
	ZINC44018332	-10.0	Polyflavonoid
	ZINC2148932	-9.9	β-carboline Alkaloid
	ZINC2156531	-9.9	Indoles Alkaloid
	ZINC3197535	-9.9	Polyflavonoid
	ZINC2102620	-9.9	Indoles Alkaloid
	ZINC2123402	-9.9	β-carboline Alkaloid
	ZINC2149488	-9.9	β-carboline Alkaloid
	ZINC1531664	-9.9	Polyflavonoid
Hydroxychloroquine	**Hidroxychloroquine**	**-5.2**	**4-aminoquinoline**
	ZINC2101723	-10.2	β-carboline Alkaloid
	ZINC2094526	-9.8	β-carboline Alkaloid
	ZINC2094304	-9.6	β-carboline Alkaloid
	ZINC2091604	-9.4	β-carboline Alkaloid
	ZINC2113496	-9.4	β-carboline Alkaloid
	ZINC1460216	-9.3	Angular Pyranocoumarin
	ZINC2123008	-9.2	β-carboline Alkaloid
	ZINC682759	-9.2	Harmala Alkaloids
	ZINC2105243	-9.2	β-carboline Alkaloid
	ZINC2111696	-9.1	β-carboline Alkaloid
	N3	**-6.2**	**Peptide-like**

Preprints (www.preprints.org) | NOT PEER-REVIEWED | Posted: 1 April 2020 doi:10.20944/preprints202004.0003.v1

N3	ZINC2104482	-10.1	β-carboline Alkaloid
	ZINC3984030	-9.9	Polyflavonoid
	ZINC1531664	-9.8	Polyflavonoid
	ZINC2152199	-9.8	β-carboline Alkaloid
	ZINC4096847	-9.6	Flavonoid-3-O-glycoside
	ZINC3947428	-9.6	Flavonoid-3-O-glycoside
	ZINC2092587	-9.6	β-carboline Alkaloid
	ZINC2115924	-9.5	β-carboline Alkaloid
	ZINC2110081	-9.5	Lupin Alkaloid
	ZINC1898165	-9.5	Benzofuran